

Causal Fourier Analysis on Directed Acyclic Graphs and Posets

Bastian Seifert, *Member, IEEE* Chris Wendler, *Student Member, IEEE* Markus Püschel, *Fellow, IEEE*

Abstract—We present a novel form of Fourier analysis, and associated signal processing concepts, for signals (or data) indexed by edge-weighted directed acyclic graphs (DAGs). This means that our Fourier basis yields an eigendecomposition of a suitable notion of shift and convolution operators that we define. DAGs are the common model to capture causal relationships between data values and in this case our proposed Fourier analysis relates data with its causes under a linearity assumption that we define. The definition of the Fourier transform requires the transitive closure of the weighted DAG for which several forms are possible depending on the interpretation of the edge weights. Examples include level of influence, distance, or pollution distribution. Our framework is different from prior GSP: it is specific to DAGs and leverages, and extends, the classical theory of Moebius inversion from combinatorics. For a prototypical application we consider DAGs modeling dynamic networks in which edges change over time. Specifically, we model the spread of an infection on such a DAG obtained from real-world contact tracing data and learn the infection signal from samples assuming sparsity in the Fourier domain.

Index Terms—Graph signal processing, DAG, partial order, causality, structural equation model, Moebius inversion, Fourier transform, convolution, non-Euclidean, Fourier sparsity, dynamic graph, infection spreading, binary classifier

I. INTRODUCTION

Causality studies which events influence others building on powerful classical theories including Bayesian networks and structural causal models [1], [2]. However, understanding and deriving causality from data continues to be a challenging problem in data science and machine learning [3]. The common index domains for causal data are directed acyclic graphs (DAGs), in which the nodes represent events and the directed edges causal relationships. Motivated by their importance, we propose a novel form of Fourier analysis for signals (or data) on DAGs, including associated signal processing (SP) concepts of shift, convolution, spectrum, frequency response, and others. DAGs are closely related to partially ordered sets (posets), where the partial order determines whether a node is a predecessor of another node. Thus, our SP framework can equivalently be considered for signals on posets.

Our framework is specific for DAGs and fundamentally different from prior graph SP based on adjacency matrix or Laplacian [4], [5], which fails for DAGs due to a collapsing spectrum. The causal nature of our framework is reflected in both shift and associated Fourier transform as will become clear later. Before we state our contribution in greater detail we provide the context of related work.

Graph signal processing. Graph SP is concerned with signals indexed by the nodes of a graph and generalizes classical SP concepts by choosing adjacency matrix or Laplacian, or variants thereof as shift (or variation) operator [4], [5], which is known to be the defining concept of any linear SP framework [6]. For undirected graphs, the eigendecomposition of the shift exists and yields an orthogonal Fourier transform; other SP concepts and techniques take meaningful forms [7]. For directed graphs (digraphs) a proper generalization is still considered an open problem [7, Sec. III.A], since an eigendecomposition does not exist in general and the more general Jordan normal form is not computable. DAGs constitute, in a sense, a worst case among digraphs since the adjacency shift has only one eigenvalue zero.

Several solutions have been proposed for digraphs. One computes a Fourier basis that minimizes the sum of directed variations [8], or evenly spreads them [9], [10]. Others include changing the shift to the Hermitian Laplacian [11], using an approximation based on the Schur decomposition [12], or adding generalized boundary conditions, i.e., additional edges to the digraph [13]. All these are fundamentally different from our approach which is specific to acyclic digraphs and based on a very different notion of shift and Fourier basis.

Causality. Classical models for causality include Bayesian networks [1], which encode multivariate probability distributions and enable different forms of causal reasoning. Structural causal models (SCMs), also called structural equation models (SEMs) [2], define how variables are computed from predecessors. Both approaches are probabilistic and model data as random vectors on DAGs, in which the edges represent causal dependencies. Granger causality [14] considers concurrent time series and investigates whether the past values of one are capable of predicting future values of another by fitting a suitably designed autoregressive model, so it does not capture true causality. Despite powerful theory, learning causality from data is hard with many pitfalls [15], [16], [3]. In particular, causal data typically has a DAG as index domain, but the converse does not hold: if data is given on a DAG, its edges do not generally imply causal relationships due to possible confounding variables, and detecting causality does require techniques such as interventions [2].

Our proposed framework is non-probabilistic and linear and has a different objective: it aims to bring a suitable form of Fourier analysis and associated concepts to data that is indexed by a DAG (or poset), whether the DAG captures causality or not. However, in the causal case, and under a linearity assumption that we will define, our Fourier analysis relates signal values to its causes. Further, there is a relation to the special class of linear SEMs that we explain in detail later.

The authors are with the Department of Computer Science, ETH Zurich, Switzerland (email: seifert.bastian@protonmail.com, chris.wendler@inf.ethz.ch, pueschel@inf.ethz.ch)

Manuscript received ???; revised ???

SP on non-Euclidean domains. Besides graph SP, other SP frameworks for non-Euclidean domains have been proposed.

One line of work is topological SP [17] based on the Hodge Laplacian, which considers signals defined on simplicial complexes, with values assigned to nodes, edges, or higher-order faces. The framework was generalized to cell complexes in [18], [19].

Hypergraphs generalize graphs by allowing edges with more than two nodes. A topological approach to hypergraph SP similar to above was proposed in [20], whereas [21] uses the adjacency tensor and tensor decomposition to define a notion of spectrum, sampling theory, and filters.

Quiver SP [22] considers directed multigraphs (i.e., multiple directed edges between the same nodes are possible), and develops an SP theory based on the rich representation theory of these structures.

Graphon SP is a continuous extension of SP on undirected graphs, thus enabling sampling among other things [23].

Direct predecessors of our work is SP on powersets, i.e., with set functions [24], [25], and SP on meet/join lattices [26], [27], [28]. Both are very special cases of posets (or DAGs) and constitute special cases of the framework proposed in this paper. Here, we generalize this prior work significantly in two dimensions. First, from the special class of meet/join lattices to arbitrary posets, which then makes it applicable to arbitrary DAGs and relates our Fourier analysis to causal data. Second, we allow for edge weights in the DAGs, which is crucial for broader applicability. We presented an initial step towards the first generalization in [29].

Several of the above generalized SP frameworks, and the work in this paper, build on the algebraic signal processing theory, which provides the axioms, insights, and derivation guidelines for any linear SP framework [6], [30] and was used to consider the first shifts beyond standard translation/delay [31], [32], [33].

Contribution. We present a novel form of Fourier analysis, and associated basic SP concepts, for signals (or data) indexed by the nodes of a weighted DAG, extending and completing our preliminary work in [29]. The Fourier basis is the eigenbasis of associated shift and convolution operators that we define, and also yields an associated notion of frequency response. The framework is specific to DAGs and cannot be used for arbitrary directed graphs.

If the DAG captures causal relationships between nodes then our Fourier analysis relates signal values with causes under a linearity assumption that we define. However, our work cannot be used to detect causal relationships, which is a hard problem [2] but, instead, is intended to provide a meaningful form of Fourier analysis (and associated convolution) to signals on DAGs, whether they capture causal relationships or not.

Our framework requires the weighted transitive closure of the given DAG as the first step. We discuss possible choices of weights and their interpretation, which include level of influence, pollution distribution, or distance. The closure also makes DAGs equivalent to weighted posets and thus our work can be used for signals on any partially ordered index domain. We show that in contrast to discrete-time SP and graph SP, the

spectrum is only partially ordered, isomorphic to the partial order of the index domain.

One possible application domain are dynamic networks whose edges change over time, which can be modeled as DAGs by unrolling the time dimension and connecting subsequent iterations of the graphs accordingly. As a prototypical experiment we first model the spread of a disease on such a DAG, which is derived from real-world contact tracing data that captures distances between people along time. Then we learn such an infection signal from a restricted number of samples under the assumption of sparsity in the Fourier domain, a property that we will motivate. Our causal Fourier basis yields superior results when compared to prior graph Fourier bases, which require dropping the directionality of the edges.

II. DAGS AND POSETS

We explain the necessary background on directed acyclic graphs (DAGs), partially ordered sets (posets), and their close relationship.

DAGs. A directed graph (digraph) $D = (V, E)$ consists of a finite set V of n nodes and a set E of m directed edges: $E \subseteq \{(x, y) \mid x, y \in V\}$. D is acyclic, and thus a DAG, if it contains no cycles. Since D is acyclic, we can sort V topologically, which means $(x, y) \in E$ implies that y comes after x . We consider weighted DAGs (V, E, A) , in which each edge (x, y) is assigned a nonzero weight $a_{x,y}$, which are collected in the matrix

$$A = (a_{x,y})_{x,y \in V} = \begin{cases} a_{x,y} & \text{if } (x, y) \in E, \\ 0 & \text{otherwise.} \end{cases} \quad (1)$$

The topological sort makes A upper triangular with zeros on the diagonal. If all weights are $= 1$, A is just the adjacency matrix.

Posets. A partially ordered set (poset) [34] is a finite set P with a partial order, i.e., a binary relation \leq that satisfies for all $x, y, z \in P$

- 1) $x \leq x$ (reflexivity),
- 2) $x \leq y$ and $y \leq x$ implies $x = y$ (antisymmetry),
- 3) $x \leq y$ and $y \leq z$ implies $x \leq z$ (transitivity).

We write $x < y$ if $x \leq y$ but $x \neq y$. An element $y \in P$ covers $x \in P$ if $x < y$ and there is no $z \in P$ with $x < z < y$.

Relation between DAGs and Posets. Every DAG $D = (V, E)$ induces a unique partial order on V , defined as $x < y$ if x is a predecessor of y , i.e., if there is a path from x to y .

Conversely, for a given poset P there are several DAGs that induce it, but two are special and unique. One is the *reachability* graph $\overline{D} = (P, \overline{E})$ with $\overline{E} = \{(x, y) \mid x < y\}$. This DAG is *transitively closed*, i.e., whenever there is a path from x to y there is also an edge (x, y) . We mark this property with an overline. The other unique DAG inducing P is the *cover graph* $D = (P, E)$ with $E = \{(x, y) \mid y \text{ covers } x\}$. This graph is *transitively reduced*, i.e., the DAG with the fewest number of edges inducing P . It contains no edge (x, y) if there is another path from x to y in D .

Example. In Fig. 1 we show an example of a DAG together with its transitive reduction and its transitive closure. All three DAGs induce the same poset.

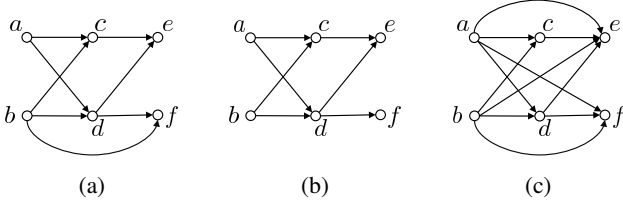


Fig. 1: (a) A DAG D , (b) its transitive reduction, and (c) its transitive closure \overline{D} . All three induce the same poset for which (b) is the cover graph, and (c) the reachability graph.

In summary, every DAG uniquely defines a poset, whereas a poset can be represented by several DAGs. These however, have the same transitive reduction or transitive closure. We discussed the equivalence of posets and DAGs only in the case of trivial weights $= 1$. For our novel Fourier analysis we will need an extension to the weighted case in the next section, in particular of the concept of transitive closure.

III. SIGNAL MODEL AND WEIGHTED TRANSITIVE CLOSURES

DAGs are a common model to represent events and their causal relationships, e.g., in the probabilistic theory of Bayesian networks [1], to efficiently represent and work with multivariate probability distributions. However, if data is indexed by a DAG its edges generally do not imply causality due to possible confounding variables [2]. Here, we build a non-probabilistic linear model and an associated Fourier analysis for data, or signals, on DAGs, whether its edges capture causal relationships or not. However, we will use the term “cause” below since, if the DAG does capture causality, and under a linearity assumption that we define, our Fourier analysis relates signal values to their causes.

We first define the basic structure of our model and identify the need for a weighted transitive closure for which we then provide several intuitive variants. With these concepts in place, we will then define for DAGs novel forms of basic SP concepts including shift, convolution, and Fourier transform, frequency response, and others, in the next section.

A. Basic signal model

We assume a given weighted DAG $D = (V, E, A)$ with induced partial order \leq on V , $|V| = n$. We consider signals on D as column vectors of the form

$$\mathbf{s} = (s_x)_{x \in V} \in \mathbb{R}^n,$$

where the order of the s_x is determined by the topological sort of V .

We call each $x \in V$ an event and say that an event y is a cause of the event x if $y \leq x$. Further, we assume that every event $y \in V$ is associated with an unknown cost (or contribution) $c_y \in \mathbb{R}$ and that the (measured) signal value at $x \in V$ is given by a weighted sum of the costs of the causes:

$$s_x = \sum_{y \leq x} w_{y,x} c_y, \quad x \in V. \quad (2)$$

Intuitively, the weights determine the influence of the causes for an event. Collecting the $w_{y,x}$ in a sparse matrix yields the equivalent form

$$\mathbf{s} = W^T \mathbf{c}, \quad (3)$$

where we use the transpose for indexing analogous to A in (1).

By (slight) abuse of notation we also say that c_y , for $y \leq x$, is a cause of s_x .

As a simple example, consider a river network, where pollution s_x is measured at finitely many locations $x \in V$ and that is polluted with unknown intensity c_y at a subset of these locations. The weights could quantify the water flow between locations or the degree of sedimentation (loss) of pollution between locations.

The question now is, given D , how to define the weights in W in a reasonable and intuitive way. The weight matrix A provides some weights but, unless transitively closed, not all that are needed for the complete equation in (2). In particular, $w_{y,x}$ for $(y, x) \in \overline{E} \setminus E$ needs to be defined. We will see that there are choices.

On the use of the term “cause”. We use the term cause since we believe it helps with understanding our model. However, we want to stress again that (2) does not imply causality but could just express a linear relation, excluding hidden, confounding variables. Thus, strictly speaking, the term “cause” for the c_y is not correct in this case. We still use it to emphasize that if (2) is a causal relationship, it does relate signal values and causes, and since it helps with understanding the different forms of transitive closure discussed next. In any event, our Fourier analysis and entire framework is applicable to any signal on any DAG.

B. Weighted Transitive Closure

For (2) we need to define $w_{y,x}$ for all $y < x$, given D , which is equivalent to computing a weighted transitive closure $\overline{D} = (V, \overline{E}, \overline{A})$ of $D = (V, E, A)$ and setting $w_{y,x} = \overline{a}_{y,x}$ for $y < x$. We propose some reasonable choices that depend on the meaning of the edge weights in A . Examples of meanings, given a pair $y < x$, include: binary (y is a cause of x or not), distance, capacity, reliability, or derivatives thereof, but many other choices are conceivable. Some of the associated closures leverage the theory from [35] as further explained below.

Trivial choice: Zero closure. The trivial choice is to simply add zero weights to edges in the transitive closure that are not yet present in D , which means setting $\overline{A} = A$. This choice makes (2) “Markovian” in the sense that the sum in (2) only contains direct predecessors in D .

Boolean weights: Standard transitive closure. If A is the adjacency matrix, i.e., has all weights $= 1$, one obvious choice is to give all edges in the transitive closure the weight 1 as well, i.e., set \overline{A} as the adjacency matrix of \overline{D} .

Pollution. The weights in A could encode what fraction of a potential pollutant inserted at a node y arrives at a successor x . Thus the weights are in $[0, 1]$ and, for each node, the sum of the weights of outgoing edges should be ≤ 1 . The transitive closure \overline{A} would then contain the same information, but now for each pair (y, x) of nodes connected by a path. The fractions

multiply along paths and have to be summed over all paths to obtain the result.

In this case there is a known formula [35], which uses that $A^n = 0$:

$$\bar{A} = A + A^2 + \dots + A^{n-1} = (I_n - A)^{-1} - I_n. \quad (4)$$

Reliability/influence. The weights in A could encode reliability or influence factors in $[0, 1]$, where $a_{y,x} = 1$ means 100% reliability of the edge or influence of y on x and $a_{y,x} = 0$ means none. Along paths, these influences multiply and $\bar{a}_{y,x}$ could encode the most reliable path from y to x .

Shortest path. The weights in A could encode distances in \mathbb{R}^+ between nodes. In this case, the weights $\bar{a}_{y,x}$ in \bar{A} could be defined as the shortest path from y to x in D . Since one would assume causes y that are farther from x in D to have less influence, one could consider derivatives of a path length ℓ such as $1/\ell$ or $e^{-\ell}$. The latter choice effectively converts distances to influences in the sense discussed right above.

Capacity. The weights in A could encode capacity or throughput $\in \mathbb{R}^+$ of edges. The capacity of a path is determined by the minimal capacity among its edges and $\bar{a}_{y,x}$ could encode the largest capacity path between y and x .

Computation. Various algorithms are available to compute transitive closures and their associated weights. The special cases that we just presented can be solved with one generic algorithm, instantiated in different ways [36]. We show it in its simplest form in Fig. 2; an optimized version can be found in [36]. The algorithm is initialized with the weight matrix A on which it performs n^3 iterations for a total runtime of $O(n^3)$. It is generic in the choice of addition \oplus and multiplication \otimes used, which must satisfy a semiring property (e.g., associativity, distributivity, and commutativity).

Table I shows several choices of semirings S and the associated result of the algorithm. Intuitively, \otimes determines how weights of consecutive edges are combined (e.g., product for reliability, sum for path length), and \oplus how one combines alternative paths (e.g., sum for pollution, min for shortest path length). Note that with \oplus and \otimes also the definition of 0 (neutral element for addition) and 1 (neutral element for multiplication) changes as shown in the table. E.g., for shortest path, $0_S = \infty$ since $u \oplus \infty = \min(u, \infty) = u = \infty \oplus u$. Thus, in the algorithm, zeros in A have to be replaced with ∞ upon initialization.

In essence the algorithm performs (4), but with operations from the chosen semiring. For shortest path, the algorithm is equivalent to the classical Floyd-Warshall algorithm [37].

Other choices of weighted transitive closure may require other algorithms. E.g., overall capacity between two nodes requires max-flow algorithms [38]. The related structural equation models (discussed later in Section IV-D) use the pollution model but without constraints on the weights.

Examples. Fig. 3 shows a few examples of transitive closures, using the DAG from Fig. 1(a) as starting point. Note that the transitive closure \bar{A} may overwrite weights in A . E.g., the bottom edge in Fig. 3e has weight 4.5, but after closure, the shortest path from b to f has length $3.2 = 1.5 + 1.7$.

```

function WEIGHTEDTRANSITIVECLOSURE( $W$ )
   $H^{(0)} \leftarrow A$ 
  for  $k = 1, \dots, n$  do
    for  $i = 1, \dots, n$  do
      for  $j = 1, \dots, n$  do
         $h_{(x_i, x_j)}^{(k)} \leftarrow h_{(x_i, x_j)}^{(k-1)} \oplus (h_{(x_i, x_k)}^{(k-1)} \otimes h_{(x_k, x_j)}^{(k-1)})$ 
      end for
    end for
  end for
  return  $\bar{A} = H^{(n)}$ 
end function

```

Fig. 2: Generic algorithm to compute various forms of weighted transitive closure in $O(n^3)$. The genericity is in the choice of addition \oplus and multiplication \otimes , which need to satisfy a semiring property. Possible choices and the associated results are shown in Table I.

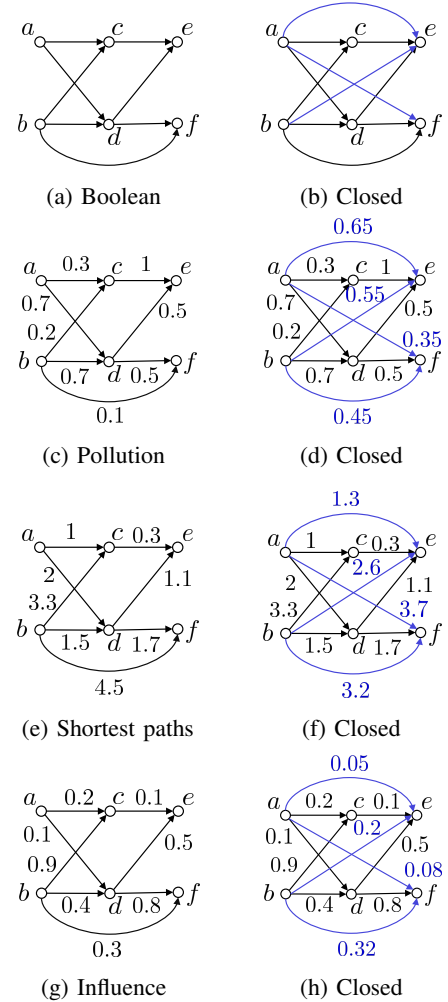


Fig. 3: Example DAG with different weights (left) and their corresponding transitive closures with respect to different models (right). The modified and added weights and edges are colored blue.

S	$u \oplus v$	$u \odot v$	0_S	1_S	Meaning of edge weight $\bar{a}_{x,y}$ in closure
$\{0, 1\}$	u or v	u and v	0	1	Reachability in graphs; x is cause of y
$[0, 1]$	$u + v$	$u \cdot v$	0	1	Fraction of pollution from x reaching y
$[0, 1]$	$\max(u, v)$	$u \cdot v$	0	1	Strongest influence/most reliable path from x to y
$\mathbb{R}^+ \cup \{\infty\}$	$\min(u, v)$	$u + v$	∞	0	Shortest path length from x to y
$\mathbb{R}^+ \cup \{\infty\}$	$\max(u, v)$	$\min(u, v)$	0	∞	Largest capacity path from x to y

TABLE I: Examples of choices for semiring operations \oplus, \otimes when operating on edge weights in the algorithm of Fig. 2. For the pollution interpretation in the second row, the weights of outgoing edges have to sum to ≤ 1 . The table is adapted from [36].

C. Reflexive closure

Finally, we need to define $w_{x,x}$ in (2), which accounts for reflexivity in the partial order, i.e., the fact that c_x is a cause of s_x . Our model requires $w_{x,x} \neq 0$, since later we want the triangular matrix W^T in (3) to be invertible. In practice we choose $w_{x,x} = 1$. For the special case of pollution, we obtain a closed form using (4):

$$W = \bar{A} + I_n = (I_n - A)^{-1}. \quad (5)$$

In three of the five cases in Table I the choice of 1 coincides with 1_S (fraction of pollution or influence of a node on itself is = 1), but poses a problem for the others. For shortest paths this suggests, for example and as we also do later, converting path length d to exponential decay e^{-d} , which makes it a particular influence model, effectively converting $(\min, +)$ to (\max, \cdot) . For capacity one could choose $e^{-1/c}$ for capacity c .

IV. CAUSAL FOURIER ANALYSIS ON DAGS

Given a weighted DAG $D = (V, E, A)$, we assume we have decided on a suitable transitive/reflective closure W of A as explained in Section III. We restate our signal model, which assumes that a signal on D is a linear combination of unknown causes¹ associated with the nodes:

$$s_x = \sum_{y \leq x} w_{y,x} c_y \quad \text{or} \quad \mathbf{s} = W^T \mathbf{c}. \quad (6)$$

In this section we will build on this equation to develop a linear SP framework for signals on DAGs. In short, we will argue that \mathbf{c} can be interpreted as a form of spectrum of \mathbf{s} , with W^{-T} as associated Fourier transform. We do so following the general theory in [6], [30]: we define a suitable notion of shift and convolution for which the columns of W^T form a joint eigenbasis. Our derivations leverage the classical theory of Moebius inversion from combinatorics [39], which is concerned with equations on posets of the form in (6). We start by inverting (6).

A. Calculating Causes: Moebius Inversion

For trivial weights $w_{y,x} = 1$, calculating \mathbf{c} from \mathbf{s} is the classical Moebius inversion from [39]. The extension to arbitrary weights needed here is straightforward and provides a formula for W^{-T} .

¹Again, we remind the reader that the term “cause” is, strictly speaking, only correct if the relationship in (6) is causal, i.e., there are no hidden confounding variables [2]. Our proposed Fourier analysis, and the related concepts we introduce, can be applied regardless.

Theorem 1

$$s_x = \sum_{y \leq x} w_{y,x} c_y, \text{ if and only if } c_y = \sum_{x \leq y} \mu_w(x, y) s_x. \quad (7)$$

Here μ_w is the weighted Moebius function, recursively defined as

$$\begin{aligned} \mu_w(x, x) &= 1, & \text{for } x \in V, \\ \mu_w(x, y) &= - \sum_{x \leq z < y} w_{z,y} \mu_w(x, z), & \text{for } x \neq y. \end{aligned}$$

We provide a proof in the appendix.

B. From Shift to Fourier Transform

Causal shifts. For every $q \in V$ we define a shift on \mathbf{s} as

$$(T_q \mathbf{s})_x = \sum_{y \leq x \text{ and } y \leq q} w_{y,x} c_y \text{ for all } x \in V. \quad (8)$$

In words, comparing to (6), the result is the signal with all causes removed, which are not common causes of q and x . We consider it as a *causal delay* of \mathbf{s} by q .

But to obtain a proper representation of the shift, we need to express the right-hand side of (8) as linear combination of signal values. First, we assume the very special case of all weights $w_{y,x} = 1$ and that x and q have an unique greatest lower bound in D denoted with $x \wedge q$, i.e.: for all $y \neq x \wedge q$ with $y \leq x$ and $y \leq q$ we have $x \wedge q < y$. Using it in (8) yields

$$(T_q \mathbf{s})_x = s_{x \wedge q}, \quad (9)$$

which, in a sense, formally captures a form of “causal delay” by q .

In the general case, the greatest lower bound is not unique. Consider again trivial weights and g and h in Fig. 4, which requires a summation over the causes $a-f$. s_d, s_e, s_f sum over the blue, red and yellow parts, which means when summing them the causes $a-c$ are considered thrice which requires a subtraction of two times s_b and s_c , and thus a final addition of s_a , a form of inclusion-exclusion in set theory [34, Chap. 2].

In general, also the weights have to be considered and we obtain the concrete formula for T_q by inserting c_y from (7) in (8):

$$(T_q \mathbf{s})_x = \sum_{y \leq x \text{ and } y \leq q} w_{y,x} \sum_{z \leq y} \mu_w(z, y) s_z. \quad (10)$$

The shifts commute since they only affect the range of summation, and are in general not invertible. Further, they are idempotent, i.e., $T_q \circ T_q = T_q$.

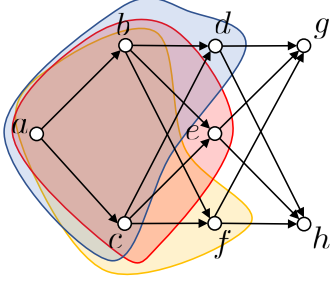


Fig. 4: Shifting \mathbf{s} with T_h associates the common causes of h and g to the shifted signal value $(T_h \mathbf{s})_g$.

Filters and convolution. The shifts generate the algebra (ring and vector space) of filters, which defines the associated notion of convolution [6]. Here, because of idempotency, the most general filter is $\sum_{q \in V} h_q T_q$ for $h_q \in \mathbb{R}$ and thus, for $\mathbf{h} \in \mathbb{R}^n$,

$$\mathbf{h} * \mathbf{s} = \left(\sum_{q \in V} h_q T_q \right) \mathbf{s}. \quad (11)$$

Since shifts commute, filters are shift-invariant, i.e., $\mathbf{h} * T_q \mathbf{s} = T_q (\mathbf{h} * \mathbf{s})$ for all $q \in V$.

Fourier basis and transform. The Fourier basis consists of the joint eigenvectors of all T_q and thus all filters. Its derivation is simple due the definition of T_q in (8), which is a pointwise multiplication on \mathbf{c} . In matrix form, using $\mathbf{s} = W^T \mathbf{c}$,

$$T_q \mathbf{s} = W^T D_q \mathbf{c}, \quad D_q = \text{diag}_{y \in V} (\iota_{\{y \leq q\}}), \quad (12)$$

where $\iota_{\{y \leq q\}}$ is the indicator function

$$\iota_{\{y \leq q\}} = \iota_{\{y \leq q\}}(y, q) = \begin{cases} 1 & \text{if } y \leq q, \\ 0 & \text{else.} \end{cases} \quad (13)$$

Using $\mathbf{s} = W^T \mathbf{c}$ in (12) shows that for all $\mathbf{c} \in \mathbb{R}^n$ we have $T_q W^T \mathbf{c} = W^T D_q \mathbf{c}$, and thus

$$T_q W^T = W^T D_q,$$

which yields the Fourier basis:

Theorem 2 (Fourier basis) *The columns of W^T from a simultaneous eigenbasis of all shifts and filters, i.e., the Fourier basis vectors are*

$$\mathbf{f}^y = (\iota_{\{y \leq x\}} w_{y,x})_{x \in V}, \quad y \in V. \quad (14)$$

The associated Fourier transform is obtained by inversion:

Theorem 3 (Fourier transform) *The Fourier transform associated with the above Fourier basis is given by*

$$\hat{\mathbf{s}} = \mathbf{c} = W^{-T} \mathbf{s} = \mathcal{F}_D \mathbf{s},$$

with Fourier transform matrix

$$\mathcal{F}_D = W^{-T} = [\mu_w(y, x) \iota_{\{x \leq y\}}]_{y, x \in V}.$$

Frequency response and convolution theorem. Equation (12) shows the frequency response of a shift T_q as the diagonal of D_q . Thus, for a general filter $H = \sum_{q \in V} h_q T_q$, it is given by

$$h'_y = \sum_{q \geq y} h_q, \quad y \in V. \quad (15)$$

Hence, in our framework Fourier transform and frequency response are computed differently, which is also the case in graph signal processing and generally due to the different roles of signal and filter space [6]. Note that (15) can be inverted using (7), i.e., every frequency response is achievable with a suitable filter. In particular, the trivial filter with $h'_y = 1$, $y \in V$, i.e., $H = I_n$ is a suitable linear combination of the T_q .

Equation 15 yields the convolution theorem:

$$\widehat{\mathbf{h} * \mathbf{s}} = \mathbf{h}' \odot \hat{\mathbf{s}}, \quad (16)$$

where \odot denotes pointwise multiplication.

Fast algorithms. The definition of \mathcal{F}_D is rather complex. In practice, since the matrix and its inverse are lower triangular, the spectrum $\hat{\mathbf{s}}$ of a signal \mathbf{s} can be computed without explicitly constructing \mathcal{F}_D using a triangular solve of

$$W^T \hat{\mathbf{s}} = \mathbf{s}, \quad (17)$$

using only $O(n^2)$ operations.

In the case of unweighted (i.e., Boolean weights) DAGs the Fourier transform and its inverse can be computed using $O(nk)$ time and memory, where k is the width of the DAG, i.e., the longest antichain or maximal number of mutually non-comparable elements of the DAG [40].

Total variation and frequency ordering. We complete our framework by a suitable definition of frequency ordering. Here we follow the high-level idea used for graphs by [4], which relates frequency ordering to the shift via total variation (TV). Here, however, we have multiple shifts and thus we consider TV separately for each shift, as common for images (with two shifts: horizontal and vertical translation) and as was done in [27] for meet/join lattices.

Definition 1 *Let \mathbf{s} be a signal on D . We define the variation w.r.t. a shift by q as $\text{TV}_q(\mathbf{s}) = \|\mathbf{s} - T_q \mathbf{s}\|_2$. The total variation of \mathbf{s} is then the vector*

$$\text{TV}(\mathbf{s}) = (\text{TV}_q(\mathbf{s}))_{q \in V} \quad (18)$$

and the sum total variation is the number

$$\text{STV}(\mathbf{s}) = \sum_{q \in V} \text{TV}_q(\mathbf{s}). \quad (19)$$

We next show that the frequencies are partially ordered in a way isomorphic to the partial order induced by D , with low frequencies corresponding to the earliest causes, i.e., those that affect the most events.

Theorem 4 *We normalize \mathbf{f}^y to $\|\mathbf{f}^y\|_2 = 1$. Then*

$$\text{TV}(\mathbf{f}^y) = (\iota_{\{y \leq q\}})_{q \in V} \quad (20)$$

and thus

$$\text{STV}(\mathbf{f}^y) = \|\text{TV}(\mathbf{f}^y)\|_1 = |\{q \in V \mid y \leq q\}|. \quad (21)$$

The poset of total variations $T = \{\text{TV}(\mathbf{f}^y) \mid y \in D\}$ w.r.t componentwise comparison is isomorphic to the (unweighted) poset induced by D , i.e., $x \leq y$ if and only if $\text{TV}(\mathbf{f}^x) \leq \text{TV}(\mathbf{f}^y)$. STV provides a topological sort of the frequencies.

We provide a proof in the appendix. We also note that the frequency ordering is independent of the choice of the two norms occurring in Theorem 4.

Next we provide a numerical example for the concepts introduced and then we conclude this section by a discussion of salient aspects of our framework.

C. Example

For an example we consider the DAG in Fig. 3c. Assuming the pollution model, its closure is given by Fig. 3d, which, including the reflexive closure, yields the matrix W .

Signal and causes. The connection between a signal \mathbf{s} and its causes \mathbf{c} , $\mathbf{s} = W^T \mathbf{c}$ (inverse Fourier transform), becomes

$$\begin{bmatrix} s_a \\ s_b \\ s_c \\ s_d \\ s_e \\ s_f \end{bmatrix} = \begin{bmatrix} c_a \\ c_b \\ 0.3c_a + 0.2c_b + c_c \\ 0.7c_a + 0.7c_b + c_d \\ 0.65c_a + 0.55c_b + c_c + 0.5c_d + c_e \\ 0.35c_a + 0.45c_b + 0.5c_d + c_f \end{bmatrix}. \quad (22)$$

Fourier transform. The Fourier transform is given by $\mathcal{F} = W^{-T}$:

$$\mathcal{F} = \begin{bmatrix} 1 & 0 & 0 & 0 & 0 & 0 \\ 0 & 1 & 0 & 0 & 0 & 0 \\ -0.3 & -0.2 & 1 & 0 & 0 & 0 \\ -0.7 & -0.7 & 0 & 1 & 0 & 0 \\ 0 & 0 & -1 & -0.5 & 1 & 0 \\ 0 & -0.1 & 0 & -0.5 & 0 & 1 \end{bmatrix}. \quad (23)$$

Shifts. As an example, the shift T_e is given by the matrix

$$T_e = \begin{bmatrix} 1 & 0 & 0 & 0 & 0 & 0 \\ 0 & 1 & 0 & 0 & 0 & 0 \\ 0 & 0 & 1 & 0 & 0 & 0 \\ 0 & 0 & 0 & 1 & 0 & 0 \\ 0 & 0 & 0 & 0 & 1 & 0 \\ 0 & 0.1 & 0 & 0.5 & 0 & 0 \end{bmatrix}. \quad (24)$$

It indeed assigns common causes, e.g.,

$$\begin{aligned} (T_e \mathbf{s})_f &= 0.1s_b + 0.5s_d \\ &= 0.1c_b + 0.5(0.7c_a + 0.7c_b + c_d) \\ &= 0.35c_a + 0.45c_b + 0.5c_d, \end{aligned} \quad (25)$$

which are the common causes of e and f .

Low-pass filter. In classical discrete-time SP, a basic low-pass filter is constructed by averaging a signal with its shifted version $\frac{1}{2}(s_n + s_{n-1})_{n \in \mathbb{Z}}$. Analogously, we construct a low-pass filter by summing the trivial shift and all shifts by q , $\tilde{H} = I + \sum_{q \in V} T_q$, and normalize by the largest eigenvalue: $H = \frac{1}{|\lambda_{\max}|} \tilde{H}$.

In our example, the trivial filter I can be written as $I = -T_d + T_e + T_f$ and thus $H = T_a + T_b + T_c + 2T_e + 2T_f$ with coordinate vector $\mathbf{h} = \frac{1}{6}(1, 1, 1, 0, 2, 2)$. In matrix form it is

$$H = \frac{1}{6} \begin{bmatrix} 6 & 0 & 0 & 0 & 0 & 0 \\ 0 & 6 & 0 & 0 & 0 & 0 \\ 0.9 & 0.6 & 3 & 0 & 0 & 0 \\ 1.4 & 1.4 & 0 & 4 & 0 & 0 \\ 1.6 & 1.3 & 1 & 1 & 2 & 0 \\ 0.7 & 1.1 & 0 & 1 & 0 & 2 \end{bmatrix}. \quad (26)$$

The frequency response of this filter is $\mathbf{h}' = (1, 1, 1/2, 2/3, 1/3, 1/3)$ which shows that indeed higher frequencies (later causes) are attenuated (the highest two by $1/3$), while, in this case, the lowest two are maintained.

D. Discussion

We discuss some of the salient aspects of our causal SP framework for DAGs.

Comparison to graph SP. Graph SP [7] is in principle designed for arbitrary graphs but is problematic for the specific subclass of DAGs due to the collapse of the spectrum and thus no clear definition of Fourier basis. In contrast, our causal SP is only applicable on DAGs. The fundamental difference is best captured in the shift definition: graph shifts capture the neighbor structure, whereas our causal shifts capture the dependency structure, directly manipulating causes, i.e., values of predecessors. As a result, all derived concepts differ substantially. In particular, in our framework DAGs first need to be transitively closed and the exclusive dependency on predecessors motivated by causality makes shifts and Fourier transform triangular.

Comparison to lattice SP. Our work substantially generalizes SP on meet/join lattices [27]. These lattices are a special class of posets or DAGs, in which each two elements have a unique greatest lower bound, which yields the concise representation of the shift in (9). This paper drops this condition, which makes it applicable to arbitrary posets and thus arbitrary DAGs. Further, and equally important, we allow for non-trivial weights and thus interpretations like distance or influence, which should considerably expand applicability.

SP on posets. Our work can equivalently be interpreted as Fourier analysis for signals on weighted posets, i.e., with a weight assigned to each pair (x, y) with $x < y$.

Spectrum. The spectrum contains the causes of a signal in the sense of our model², with later causes being the higher frequencies. Thus it is not clear that basic compression or denoising by attenuating high frequencies is directly portable. Fourier-sparsity has the appealing interpretation that a signal has few causes in our model.

We have found that in chemistry, properties of molecules have been sometimes estimated by what we would call low frequencies [41], [42], [43].

Multiple shifts. Our framework is shift-invariant and based on multiple basic shifts instead of just one in graph SP. This is not uncommon: e.g., filters on images are composed from independent shifts in x and y -direction. Fundamentally, it just means that the filter space is a polynomial algebra in multiple variables [6].

Relation to structural equation models. Structural equation models (SEMs), also called structural causal models (SCMs), are one of the main tools for analyzing causal data [2], modeled as a DAG of causally dependent random variables that satisfy functional relationships. Assuming, as before, a weighted DAG $D = (V, E, A)$ with n nodes, a *linear* SEM (e.g. [44], which uses them to learn DAGs from data) is defined as $X = A^T X + N$, where $X = (X_1, \dots, X_n)^T$ is a random vector and $N = (N_1, \dots, N_n)^T$ a random noise vector, not necessarily Gaussian. Using (5) we can write it as

$$(I_n - A^T)X = N \Leftrightarrow X = W^T N = \mathcal{F}^{-1}N,$$

²And with the mentioned caveat that the term “cause” is only correct if the equation (6) really is causal and not just a correlation.

if we choose the transitive closure of the pollution model (now without restriction on the weights). In words, the noise chosen to sample the linear SEM is then, in our sense, the spectrum of the obtained signal.

For other forms of transitive closure (e.g., Table I) our model is different from SEMs.

V. APPLICATION EXAMPLE: DYNAMIC NETWORKS

Examples of real-world networks (i.e., graphs) include proximity of persons (used, e.g., for contact-tracing of infectious people during a pandemic), peer-to-peer networks between vehicles in traffic or transactions between traders in a market. However, these networks are often non-static, e.g., the edges change with time. The work in [45] shows how to encode such a dynamic network as a DAG by assigning the graphs to discrete time steps and connecting subsequent graphs.

We consider such DAGs as one possible application domain of our work and present in this section a prototypical, semi-synthetic example: we use real contact-tracing data to simulate the spread of an infection among n individuals along time. Then we try to learn this infection signal from samples under the assumption of sparsity in the Fourier domain. We presented a restricted, simplified version of this experiment using unweighted DAGs in [29].

A. Infection Spreading on Dynamic DAGs

We explain the construction of DAGs from dynamically changing graphs and the model we use to generate infection signals from contact tracing data.

Dynamic networks as DAGs. We consider a dynamic network as a collection of (undirected) graphs $G_t = (V, E_t)$ where the set of edges E_t changes with time $t \in T = \{t_1, \dots, t_m\}$. It can be modeled as a DAG $D = (V', E')$ using the idea from [45]. Namely, we make a copy of the node set for each time point, i.e., the new node set is $V' = \{(v, t) \mid v \in V, t \in T \cup \{t_{m+1}\}\}$, where t_{m+1} is an added, last time point.

Further, we connect nodes (u, t) with $(v, t+1)$ if $(u, v) \in E_t$ and always (u, t) with $(u, t+1)$ to form E' . This construction is illustrated on a small example in Fig. 5.

The Haslemere data set. We consider the dataset from [46], which uses real smartphone proximity data to obtain a dynamic network on which the spread of a disease is then modeled and analyzed. Here we aim to learn the associated signal from samples. Concretely, the proximity of $|V| = 469$ participants was measured for three days every 5 minutes between 7am and 11pm using a smartphone app, resulting in 576 time points. Due to our infection model below we remove all edges with distance > 20 meters.

Haslemere DAG. With the above construction we turn the Haslemere dynamic network into a DAG $D = (V', E')$. Since later we want to use standard graph SP as benchmark (with directions dropped), which requires an eigendecomposition of the Laplacian or adjacency matrix, we have to restrain the size of D . Thus, we sample the contact data only every hour, resulting in $|T| = 37$ time points leading to a DAG with $|V'| = 17612$ nodes and $|E'| = 24596$ edges.

Weights. At each time point the edges of the graphs G_t are weighted by the distance of the participants. We convert the distances into influences as explained in Section III-B to ensure fading with large distances in space and, through the transitive closure, in time. Concretely, DAG edges of the form $((u, t), (u, t+1))$ obtain weight 1, and edges of the form $((u, t), (v, t+1))$ obtain weight $e^{-d_{u,v}} \in [0, 1]$, where $d(u, v)$ is the distance at time t . The transitive closure is then computed using Alg. 2.

Infection signals. [46] uses the susceptible-exposed-infectious (SEI) model to simulate the spread of a disease from a number of initially infected individuals. In this model, a healthy individual is infected with a certain probability when exposed to an infected individual. Here, to make it more realistic, we include recovery and slightly extend it to a susceptible-infected-recovered (SIR) model.

Formally, from [46], the infection force $\lambda_{u,v}(t)$ from an infected individual (node) u to a non-infected individual (node) v at each time point is modeled using a cutoff exponential

$$\lambda_{u,v}(t) = \begin{cases} e^{-d_{u,v}(t)/\rho} & \text{if } d_{u,v}(t) \leq \epsilon, \\ 0 & \text{if } d_{u,v}(t) > \epsilon, \end{cases} \quad (27)$$

where $d_{u,v}(t)$ is the distance between u and v at time t , ρ the characteristic distance set to $\rho = 10$ meters, and ϵ the cutoff distance set to $\epsilon = 20$ meters. The overall infection force to a node v is then

$$\lambda_v(t) = \sum_{u \text{ infected}} \lambda_{u,v}(t), \quad (28)$$

and the probability that the individual v gets infected at time t is

$$\text{prob}_v(t) = 1 - e^{-\lambda_v(t)}. \quad (29)$$

In our extension, a person which is infected at time t recovers at time $t+5$ and is afterwards immune. The time of 5 hours is of course unrealistically short, but this is necessary due to the small number of considered time points. The exact choice is also irrelevant for our prototypical experiment.

B. Learning Fourier-Sparse Causal Signals

Using the model from Section V-A one can generate binary (values are 0 or 1) infection signals on the DAG (V', E') by starting with a small number of infected individuals at time point one and infecting individuals in subsequent time steps with the probabilities (30). Fig. 6 shows one such signal with nine initially infected individuals. Since the connectivity information (i.e., the edges of the DAG) is distracting from the signal (the infected individuals, i.e., the red dots) we will omit the edges in the following plots. Fig. 7 shows the spectrum of the signal (indexed by the same DAG because of Theorem 4, but now with edges omitted) in Fig. 6.

In this section we show how to learn such a generated infection signal from a number of samples assuming sparsity in the Fourier domain. We explain the basic approach and show results, comparing to standard graph SP for which (necessarily) we drop the direction of the DAG edges.

Learning such signals from samples is hard. First, the signals are very sparse; thus a certain number of samples is

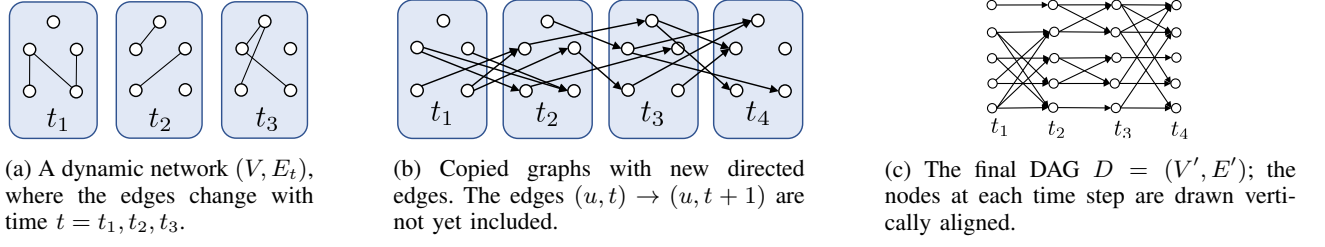


Fig. 5: Constructing a DAG from a dynamic network [45].

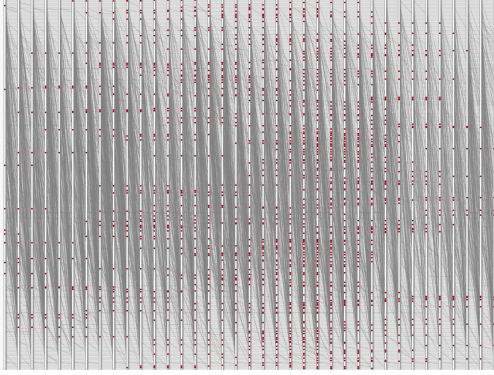


Fig. 6: One example of a generated binary infection signal with nine initially infected persons. About 9% of the values are $= 1$ (infected), the others $= 0$ (not infected).

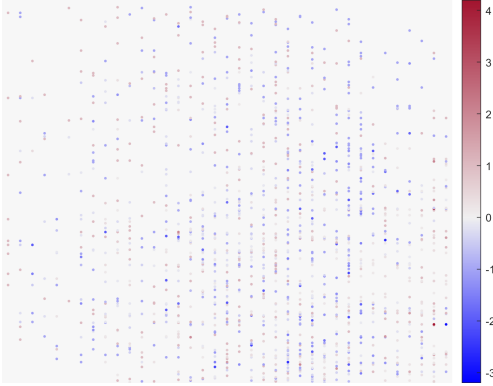


Fig. 7: Spectrum of the signal in Fig. 6. About 11% of the values are nonzero, several of which are very small.

needed to learn something about the signal at all. Second, the DAG model does not know the data generation process. In particular, the fixed recovery time is not known or used. Finally, the data generation process is stochastic in nature and hence no model can be absolute certain about the infection status after exposure and along time.

Fourier-sparse learning. The basic idea is to approximate a binary infection signal \mathbf{s} with $\tau(\sigma(\mathbf{r}))$, where \mathbf{r} is Fourier-sparse (i.e., $\hat{\mathbf{r}}$ has few nonzero values), $\sigma = 1/(1 + e^{-x})$ is the logistic sigmoid function that converts elementwise real values to probabilities, and τ is a threshold function. In our case, the default τ simply rounds elementwise to 0 or 1.

Formally, with this approximation, the probability that a

node $x \in V'$ is of class 1 (infected) is then

$$p(x) = \text{prob}(x \text{ of class } 1) = \sigma(r_x) = \sigma\left(\sum_{y \in V} \hat{r}_y f_x^y\right), \quad (30)$$

with f_x^y from (14) and $\hat{r}_y = 0$ for most $y \in V$.

We assume we observe k signal values s_1, \dots, s_k at random nodes x_1, \dots, x_k , respectively. We estimate the nonzero Fourier coefficients \hat{r}_y in (30) by solving a logistic regression problem, regularized by an L^1 -loss term to promote sparsity of $\hat{\mathbf{r}}$ [47]. The resulting optimization problem is given as

$$\min_{\hat{\mathbf{r}} \in \mathbb{R}^{|V|}} - \sum_{i=1}^k s_i \log p(x_i) + (1 - s_i) \log(1 - p(x_i)) + \lambda \sum_{y \in V} |\hat{r}_y|, \quad (31)$$

where $\lambda \ll 1$ is a hyperparameter. We found that $\lambda = 0.1$ worked well for all bases.

Experiment. We generate a set of signals as follows. We start the SIR model with $i = 5, 9, 11$ participants infected at random at time t_1 and propagate the infections as described in Section V-A. For each i we repeated the simulation ten times, resulting in 30 DAG signals overall. The signals have value 1 at node $x = (u, t)$ if the individual u is infected at time t and value 0 otherwise.

We observe a fraction $k/|V'|$ of the signal values and then use (31) with three different notions of Fourier basis to obtain a sparse $\hat{\mathbf{r}}$, which in turn determines \mathbf{r} and thus the prediction $\tau(\sigma(\mathbf{r}))$ of \mathbf{s} . For each of the three Fourier bases we consider two variants for a total of six experiments.

The three bases are our proposed basis and Laplacian/adjacency matrix GSP bases, obtained by dropping direction in the DAG (V', E') and computing eigenbases. For our basis we consider the weighted version, obtained by the transitive closure in the influence model as explained above, but also an unweighted version, obtained by a standard transitive closure (first row in Table I). For the Laplacian/adjacency matrix GSP bases we consider both the graph as is (but undirected) and its transitive closure.

All results shown are for the 30 considered signals: the respective solid lines show the mean and the shaded areas the 95% confidence interval.

Evaluation. The first idea is to compute reconstruction accuracy, computed as $1 - \|(\mathbf{s} - \tau(\sigma(\mathbf{r}))\|_2 / \|\mathbf{s}\|_2$, shown in Fig. 8 (note that the y -axis starts at 0.8, which emphasizes differences). Since the signals are binary and highly imbalanced (way more person-time combinations are non-infected than

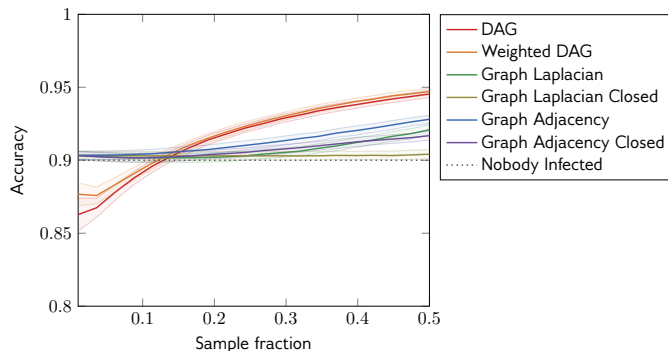


Fig. 8: Standard accuracy in the Euclidean norm is not a good measure for the quality of binary classifiers with imbalanced classes.

infected), this metric is not suitable: a trivial estimator setting every value to “nobody infected” reaches about 0.9, shown as dotted line, but cannot detect any infected node and is thus useless. More generally, binary classifiers of similar such accuracy can have vastly different quality due to differences in the number of false positives.

Thus, instead, the quality of binary classifiers with imbalanced data is measured in machine learning with the *receiver operator characteristic area under curve* (ROC-AUC) [48]. The key underlying concept is the ROC that does a cost/benefit analysis [49]. Namely, the so-called ROC curve measures how the true positive rate or TPR y (the probability of detecting an event, i.e., the benefit) changes with respect to the false positive rate or FPR x (the probability of a false alarm, i.e., the cost) by varying the classification threshold τ . A random classifier that chooses detection with probability p and not detected with probability $1 - p$ yields the ROC curve $y = x$ if p is varied in $[0, 1]$. A perfect classifier would approach the curve $y = 1$. So higher is better and the area under the ROC curve (ROC-AUC) is used as metric. The perfect classifier has AUC 1 and the trivial one (“nobody infected”) AUC 0.5.

Fig. 9 shows the ROC curves of the considered classifiers obtained with 20% sampled data. The estimation based on our proposed causal Fourier basis performs best by a large margin, compared to both GSP Fourier bases associated with the Laplacian and adjacency matrix. Transitively closing the graphs makes it worse for them. The likely reason is that the sparsity assumption does not hold with these Fourier models, whereas with our Fourier domain it indeed holds as already shown in Fig. 7. In our terminology this means relatively few causes are responsible for the signal, which the Fourier-sparse reconstruction can leverage. It shows that for the considered signals our combinatorial causal Fourier basis yields a better representation than the more geometric GSP bases.

The corresponding ROC-AUC curve used to measure the benefit in ROC curves is shown in Fig. 10. It plots the AUC of the ROC lines as function of the fraction of data points sampled (higher is better). For the sample fraction of 20% the values correspond to Fig. 9.

The superiority of our classifier compared to the benchmarks also becomes evident when looking at the reconstructed

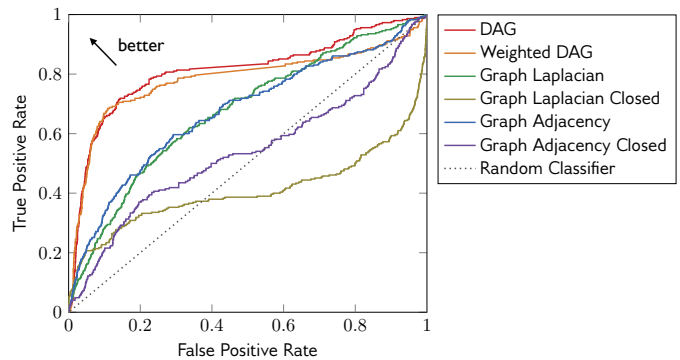


Fig. 9: Receiver operation characteristics (ROC) curves for the above sample data and the classifiers with a sample of 20% node data.

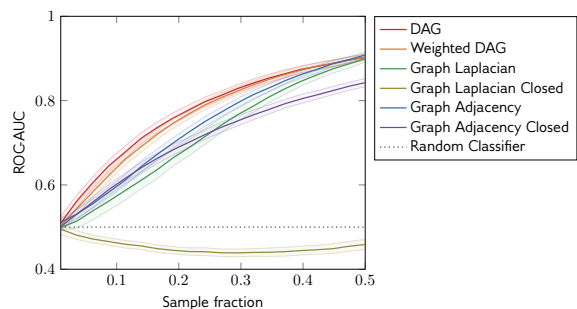


Fig. 10: Results of the proposed sparse learning approach on the Haslemere signals in the ROC-AUC metric as a function of the sample fraction.

signals. Fig. 11 shows an example with the original signal shown in Fig. 11(g). We observe that the sparsity in the Laplacian/adjacency matrix-based reconstructions appears random, whereas for our novel DAG-based method the signals have structure as often values along time steps (horizontally) tend to stay constant which captures the causal nature of the infection signal.

VI. CONCLUSION

We presented a novel linear SP framework including shift, convolution, and Fourier analysis for signals on DAGs, or, equivalently, posets. Doing so is significant both theoretically and practically. On the fundamental side we fill a blind spot in graph SP, for which digraphs are problematic and DAGs are a worst case. For applications, DAGs are the natural index domain for causal data, in which each data point causally depends on the values of predecessors. We argue that if this causal dependency is linear, and with coefficients obtained by a suitable transitive closure of the DAG, the signal and causes can be viewed as a Fourier pair. If the linear relation is not causal our proposed Fourier analysis is still mathematically sound but the spectrum cannot be interpreted as causes.

Importantly, our framework allows for edge-weighted DAGs, and, different from other non-Euclidean SP frameworks, there is a degree of freedom in their interpretation and thus the transitive closure needed to obtain a Fourier basis.



Fig. 11: Examples of reconstructed signals from a sample of 20% of the node data, using the described classifier with $\tau = 0.5$.

One particular application domain are DAGs obtained from dynamic graphs evolving over discrete time. We show an example of learning infection signals on such a graph from few samples by assuming Fourier-sparsity.

Overall, our work leverages but also extends the classical theory of Moebius inversion to define a new notion of Fourier analysis for use in signal processing and learning.

ACKNOWLEDGEMENTS

We thank Panagiotis Misiakos for the insight on the relationship between structural equation models and our novel Fourier analysis for DAGs.

REFERENCES

- [1] D. Koller and N. Friedman, *Probabilistic Graphical Models*, MIT Press, Cambridge, MA, 2009.
- [2] J. Peters, D. Janzing, and B. Schölkopf, *Elements of Causal Inference*, MIT Press, Cambridge, MA, 2017.
- [3] B. Schölkopf, “Causality for machine learning,” in *Probabilistic and Causal Inference: The Works of Judea Pearl*, pp. 765–804, 2022.
- [4] A. Sandryhaila and J. M. F. Moura, “Discrete signal processing on graphs,” *IEEE Trans. Signal Proc.*, vol. 61, no. 7, pp. 1644–1656, 2013.
- [5] D. Shuman, S. K. Narang, P. Frossard, A. Ortega, and P. Vandergheynst, “The emerging field of signal processing on graphs: Extending high-dimensional data analysis to networks and other irregular domains,” *IEEE Signal Process. Mag.*, vol. 30, no. 3, pp. 83–98, 2013.
- [6] M. Püschel and J. M. F. Moura, “Algebraic signal processing theory: Foundation and 1-D time,” *IEEE Trans. on Signal Processing*, vol. 56, no. 8, pp. 3572–3585, 2008.
- [7] A. Ortega, P. Frossard, J. Kovacevic, J. M. F. Moura, and P. Vandergheynst, “Graph Signal Processing: Overview, Challenges, and Applications,” *Proc. IEEE*, vol. 106, no. 5, pp. 808–828, 2018.
- [8] S. Sardellitti, S. Barbarossa, and P. di Lorenzo, “On the Graph Fourier Transform for Directed Graphs,” *IEEE J. Sel. Topics Signal Process.*, vol. 11, no. 6, pp. 796–811, 2017.
- [9] R. Shafipour, A. Khodabakhsh, G. Mateos, and E. Nikolova, “Digraph Fourier Transform via Spectral Dispersion Minimization,” in *Proc. Int. Conf. Acoust., Speech, and Signal Process. (ICASSP)*, 2018, pp. 6284–6288.
- [10] R. Shafipour, A. Khodabakhsh, G. Mateos, and E. Nikolova, “A Directed Graph Fourier Transform with Spread Frequency Components,” *IEEE Trans. Signal Proc.*, vol. 67, no. 4, pp. 946–960, 2019.
- [11] S. Furutani, T. Shibahara, M. Akiyama, K. Hato, and M. Aida, “Graph Signal Processing for Directed Graphs based on the Hermitian Laplacian,” in *Proc. European Conference on Machine Learning and Principles and Practice of Knowledge Discovery in Databases (ECML PKDD)*, 2019, pp. 447–463.
- [12] J. Domingos and J. M. F. Moura, “Graph Fourier Transform: A Stable Approximation,” *IEEE Trans. on Signal Process.*, vol. 68, pp. 4422–4437, 2020.
- [13] B. Seifert and M. Püschel, “Digraph Signal Processing with Generalized Boundary Conditions,” *IEEE Trans. Signal Proc.*, vol. 69, pp. 1422–1437, 2021.
- [14] C. W. J. Granger, “Investigating causal relations by econometric models and cross-spectral methods,” *Econometrica*, vol. 37, no. 3, pp. 424–438, 1969.
- [15] M. J. Vowles, N. C. Camgoz, and R. Bowden, “D’ya like DAGs? A Survey on Structure Learning and Causal Discovery,” arXiv preprint arXiv:2103.02582, 2021.
- [16] R. Guo, L. Cheng, J. Li, P. R. Hahn, and H. Liu, “A survey of learning causality with data: Problems and methods,” *ACM Computing Surveys (CSUR)*, vol. 53, no. 4, pp. 1–37, 2020.
- [17] S. Barbarossa and S. Sardellitti, “Topological signal processing over simplicial complexes,” *IEEE Trans. on Signal Processing*, vol. 68, pp. 2992–3007, 2020.
- [18] T. M. Roddenberry, M. T. Schaub, and M. Hajj, “Signal processing on cell complexes,” arXiv preprint arXiv:2110.05614, 2021.
- [19] S. Sardellitti, S. Barbarossa, and L. Testa, “Topological signal processing over cell complexes,” arXiv preprint arXiv:2112.06709, 2021.
- [20] S. Barbarossa and M. Tsitsvero, “An introduction to hypergraph signal processing,” in *Proc. Int. Conf. Acoust., Speech, and Signal Process. (ICASSP)*, 2016.
- [21] S. Zhang, Z. Ding, and S. Cui, “Introducing hypergraph signal processing: Theoretical foundation and practical applications,” *IEEE Internet of Things Journal*, vol. 7, no. 1, pp. 639–660, 2020.
- [22] A. Parada-Mayorga, H. Riess, A. Ribeiro, and R. Ghrist, “Quiver signal processing (qsp),” 2020.
- [23] L. Ruiz, L. F. O. Chamon, and A. Ribeiro, “Graphon signal processing,” *IEEE Trans. Signal Proc.*, vol. 69, pp. 4961 – 4976, 2021.
- [24] M. Püschel, “A Discrete Signal Processing Framework for Set Functions,” in *Proc. Int. Conf. Acoust., Speech, and Signal Process. (ICASSP)*, 2018, pp. 1935–1968.
- [25] M. Püschel and C. Wendler, “Discrete signal processing with set functions,” *IEEE Trans. Signal Proc.*, vol. 69, pp. 1039–1053, 2021.
- [26] M. Püschel, “A Discrete Signal Processing Framework for Meet/Join Lattices with Applications to Hypergraphs and Trees,” in *Proc. Int. Conf. Acoust., Speech, and Signal Process. (ICASSP)*, 2019, pp. 5371–5375.
- [27] M. Püschel, B. Seifert, and C. Wendler, “Discrete Signal Processing on Meet/Join Lattices,” *IEEE Trans. Signal Proc.*, vol. 69, pp. 3571–3584, 2021.
- [28] B. Seifert, C. Wendler, and M. Püschel, “Wiener filter on meet/join lattices,” in *Proc. Int. Conf. Acoust., Speech, and Signal Process. (ICASSP)*, 2021, pp. 5355–5359.
- [29] B. Seifert, C. Wendler, and M. Püschel, “Learning Fourier-Sparse Functions on DAGs,” in *ICLR 2022 Workshop on the Elements of Reasoning: Objects, Structure and Causality*, 2022.
- [30] M. Püschel and J. M. F. Moura, “Algebraic signal processing theory,” *CoRR*, vol. abs/cs/0612077, 2006.
- [31] M. Püschel and J. M. F. Moura, “Algebraic signal processing theory: 1-D space,” *IEEE Trans. on Signal Processing*, vol. 56, no. 8, pp. 3586–3599, 2008.
- [32] M. Püschel and M. Rötteler, “Algebraic signal processing theory: 2-D hexagonal spatial lattice,” *IEEE Trans. on Image Processing*, vol. 16, no. 6, pp. 1506–1521, 2007.
- [33] A. Sandryhaila, J. Kovacevic, and M. Püschel, “Algebraic signal processing theory: 1-D nearest-neighbor models,” *IEEE Trans. Signal Proc.*, vol. 60, no. 5, pp. 2247–2259, 2012.
- [34] R. P. Stanley, *Enumerative Combinatorics*, vol. 1 of *Cambridge Studies in Advanced Mathematics*, Cambridge University Press, 2 edition, 2011.
- [35] D. J. Lehmann, “Algebraic structures for transitive closure,” *Theor. Comput. Sci.*, vol. 4, pp. 59–76, 1977.
- [36] S. K. Abdali and B. D. Saunders, “Transitive closure and related semiring properties via eliminants,” *Theor. Comput. Sci.*, vol. 40, pp. 257–274, 1985.
- [37] R. W. Floyd, “Algorithm 97 (SHORTEST PATH),” *Commun. ACM*, vol. 5, no. 6, pp. 345, 1962.
- [38] Goldberg A. V. and Tarjan R. E., “A new approach to the maximum-flow problem,” *Journal ACM*, vol. 35, no. 4, pp. 921–940, 1988.
- [39] G.-C. Rota, “On the foundations of combinatorial theory. I. theory of Möbius functions,” *Z. Wahrscheinlichkeitstheorie und Verwandte Gebiete*, vol. 2, no. 4, pp. 340–368, 1964.
- [40] T. Pegolotti, B. Seifert, and M. Püschel, “Fast Moebius and Zeta transforms,” arXiv preprint, 2022.
- [41] T. Ivanciuc, D. J. Klein, and O. Ivanciuc, “Posetic cluster expansion for substitution-reaction networks and application to methylated cyclobutanes,” *J. Math. Chem.*, vol. 41, no. 4, 2007.
- [42] D. J. Klein, T. Ivanciuc, A. Ryzhov, and O. Ivanciuc, “Combinatorics of Reaction-Network Posets,” *Combinatorial Chemistry & High Throughput Screening*, vol. 11, pp. 723–733, 2008.
- [43] J. Nava, V. Kreinovich, G. Restrepo, and D. J. Klein, “Discrete Taylor Series as a Simple Way to Predict Properties of Chemical Substances like Benzenes and Cubanes,” *J. Uncertain Syst.*, vol. 4, no. 3, 2010.
- [44] X. Zheng, B. Aragam, P. K. Ravikumar, and E. P. Xing, “Dags with no tears: Continuous optimization for structure learning,” in *Advances in Neural Information Processing Systems*. 2018, vol. 31, pp. 9492–9503, Curran Associates, Inc.
- [45] H. Kim and R. Anderson, “Temporal node centrality in complex networks,” *Phys. Rev. E*, vol. 85, pp. 026107–1 – 026107–8, 2012.
- [46] S. Kissler, P. Klepac, M. Tang, A. J. K. Conlan, and J. Gog, “Sparking ‘The BBC Four Pandemic’: Leveraging citizen science and mobile phones to model the spread of disease,” bioRxiv preprint, 2018.
- [47] A. Y. Ng, “Feature selection, L_1 vs. L_2 regularization, and rotational invariance,” in *Proc. Int. Conf. on Machine Learning (ICML)*, 2004, p. 78.
- [48] A. P. Bradley, “The use of the area under the ROC curve in the evaluation of machine learning algorithms,” *Pattern Recognition*, vol. 30, no. 7, pp. 1145–1159, 1997.

- [49] T. Fawcett, “An introduction to ROC analysis,” *Pattern Recognition Letters*, vol. 27, no. 8, pp. 861–874, 2006.
- [50] M. J.R. Hall, *Combinatorial Theory*, John Wiley & Sons, 1998.

APPENDIX

Proof of Theorem 1. The proof of the weighted Moebius inversion (7) generalizes the Moebius inversion in [39] and is similar to the proof of [50, Lemma 2.2.1].

First we show that

$$\sum_{z \leq y \leq x} w_{y,x} \mu_w(z, y) = \begin{cases} 1 & \text{if } z = x, \\ 0 & \text{otherwise.} \end{cases}$$

The first case holds since $w_{x,x} = 1$. For the second case,

$$\begin{aligned} \sum_{z \leq y \leq x} w_{y,x} \mu_w(z, y) &= \sum_{z \leq y < x} w_{y,x} \mu_w(z, y) + \mu_w(z, x) \\ &= \sum_{z \leq y < x} w_{y,x} \mu_w(z, y) \\ &\quad - \sum_{z \leq y < x} w_{y,x} \mu_w(z, y) \\ &= 0, \end{aligned}$$

where we used the definition of μ_w in Theorem 1.

With this we can write

$$\begin{aligned} s_x &= \sum_{z \leq x} \sum_{z \leq y \leq x} w_{y,x} \mu_w(z, y) s_z, \\ &= \sum_{y \leq x} w_{y,x} \sum_{z \leq y} \mu_w(z, y) s_z. \end{aligned}$$

Thus, the formula for c_y in Theorem 1 implies the formula for s_x , and since W^T is invertible, the reverse holds as well.

Proof of Theorem 4. Using (12), we get

$$T_q \mathbf{f}^y = \begin{cases} \mathbf{f}^y & \text{if } y \leq q, \\ 0 & \text{otherwise,} \end{cases}$$

which also holds after normalization. It follows $\text{TV}_q(\mathbf{f}^y) = \|\mathbf{f}^y - T_q \mathbf{f}^y\|_2 = 1$ if $y \not\leq q$ and $= 0$ otherwise, which yields (20) and (21).

For the isomorphic partial ordering assume first $x \leq y$ for $x, y \in V$. Then $y \leq q$ implies $x \leq q$, i.e., $x \not\leq q$ implies $y \not\leq q$. It follows $\text{TV}_q(\mathbf{f}^x) \leq \text{TV}_q(\mathbf{f}^y)$.

For the reverse assume $\text{TV}(f^x) \leq \text{TV}(f^y)$, i.e., $\text{TV}_q(\mathbf{f}^x) \leq \text{TV}_q(\mathbf{f}^y)$ for all $q \in V$. It follows that $x \not\leq q$ implies $y \not\leq q$, i.e., that $y \leq q$ implies $x \leq q$. Setting $q = y$ yields the result.